Biophysical Chemistry 147 (2010) 140–145

Contents lists available at ScienceDirect

Biophysical Chemistry

journal homepage: http://www.elsevier.com/locate/biophyschem

Formation of Schiff-base for photoreaction mechanism of red shift of GFP spectra

Jun Koseki, Yukiumi Kita, Masanori Tachikawa *

Quantum Chemistry Division, Graduate School of Science, Yokohama City University, 22-2 Seto, Kanazawa-ku, Yokohama 236-0027, Japan

ARTICLE INFO

Article history:
Received 30 November 2009
Received in revised form 16 January 2010
Accepted 20 January 2010
Available online 1 February 2010

Keyword:
Red shift of green fluorescent protein spectra
Formation of Schiff-base
Absence of oxygen
Irreversible photoreaction

ABSTRACT

We have proposed the formation of Schiff-base between R96 and chromophore (CRO) to elucidate the reaction mechanism for the irreversible red shift of green fluorescent protein (GFP) spectra under the absence of oxygen. The difference between absorption energies of reactant and product for our GFP models with CIS(D)/6-31G* level is 0.21 eV, which is in reasonable agreement with the corresponding experimental value of 0.25 eV. We have suggested the irreversible photoreaction mechanism, where the CRO excited from ground (S_0) state to first excited singlet (S_1) state immediately turns to the first excited triplet (T_1) state, and the nucleophilic addition reaction occurs on the T_1 state.

© 2010 Elsevier B.V. All rights reserved.

1. Introduction

Green fluorescent protein (GFP) is one of the fluorescent proteins, discovered from jellyfish (*Aequorea victoria*) by Shimomura et al. [1] as companion protein to aequorin in 1960's. Many mutants that emit fluorescence at different wavelengths have been discovered and created [2]. A GFP and many mutants have β-can structures, where a chromophore (CRO) is in the center of β-barrel as shown in Fig. 1. Absorption and fluorescent wave lengths of fluorescent proteins strongly depend on the CRO structures [3]. It has been reported that hydrogen-bonded network around the CRO and excited state proton transfer (ESPT) are very important for absorption and emission in fluorescent protein [4–8]. It has been also reported that production and decay of the fluorescent state occur via totally symmetric and out of plane modes [10–13]. Nowadays, these fluorescent proteins are applied as a biological marker in the wide area such as molecular biology, medicine, and cell biology [9].

Wild-type (Wt-) GFP has a major absorption peak at 398 nm (neutral state of CRO) and a minor absorption peak at 475 nm (anionic state of CRO). The emissions of neutral and anionic state of CRO are almost the same peak at 503–508 nm. Under the absence of oxygen, on the other hand, the irreversible red shift of absorption and fluorescent spectra of GFP was found by Elowitz et al. [14,15] with brief pulses of 488 nm light, which is the same wave length of GFP absorption one. The absorption and emission bands for RsFP (the GFP after photoactivation) are observed at 525 nm and 600 nm, respectively. To our knowledge, however, the mechanism for this red-shift photoreaction and the structure of RsFP are not known, yet. In the practical viewpoint, such photoactivation detracts from the proper sorting of some cells, and be fatal flaw when the cell-stress is observed under the absence of oxygen.

Meanwhile, there are many red fluorescent proteins such as DsRED [16] and KAEDE [17] etc., which have the conjugated double bonding at residues adjacent to CRO. With a similar manner, we would like to propose the elongation of the conjugated double bonding for the structure of RsFP to reproduce the red-shift of GFP spectra. The CRO in GFP can have some possible points [18] for the elongation of the conjugation, at OH-group on phenol ring, at residues adjacent to CRO, and at imidazole carbonyl group. It is well known that such red-shift occurs in not only Wt-GFP but also some its mutants, S65T, E222G, T203I, etc. [9] where S65T and E222G have only anionic states of CRO ($-O^-$ on phenol ring), and T203I has only a neutral state of CRO (–OH on phenol ring). These geometrical information for GFP and its mutants show that this photoreaction is independent on whether the state of CRO is neutral or anionic. For this reason, there is no possibility that the conjugated double bonding is elongated from OH-group on phenol ring. On the other hand, since the red-shift is also observed in the mutant S65T, in which the residue adjacent to CRO is replaced, there is no possibility that the conjugated double bonding is elongated from residues adjacent to CRO. Thus, we would like to pay attention at imidazole carbonyl group of CRO for the red-shift of GFP, and propose the formation of Schiff-base between R96 and CRO.

In this paper, we have performed *ab initio* molecular orbital (MO) and molecular dynamics (MD) calculations to elucidate the red-shift mechanism of irreversible photoreaction for GFP. In Section 2, we describe the reaction scheme and the CRO models, and computational details of MO and MD calculations. The results of our calculations are reported in Section 3. To explore the structure after photoreaction, we have proposed the model structures of CRO and validated them with MO calculation. We have analyzed photoreaction with MO and MD

* Corresponding author.
E-mail address: tachi@yokohama-cu.ac.jp (M. Tachikawa).

0301-4622/$ – see front matter © 2010 Elsevier B.V. All rights reserved.
doi:10.1016/j.bpc.2010.01.008

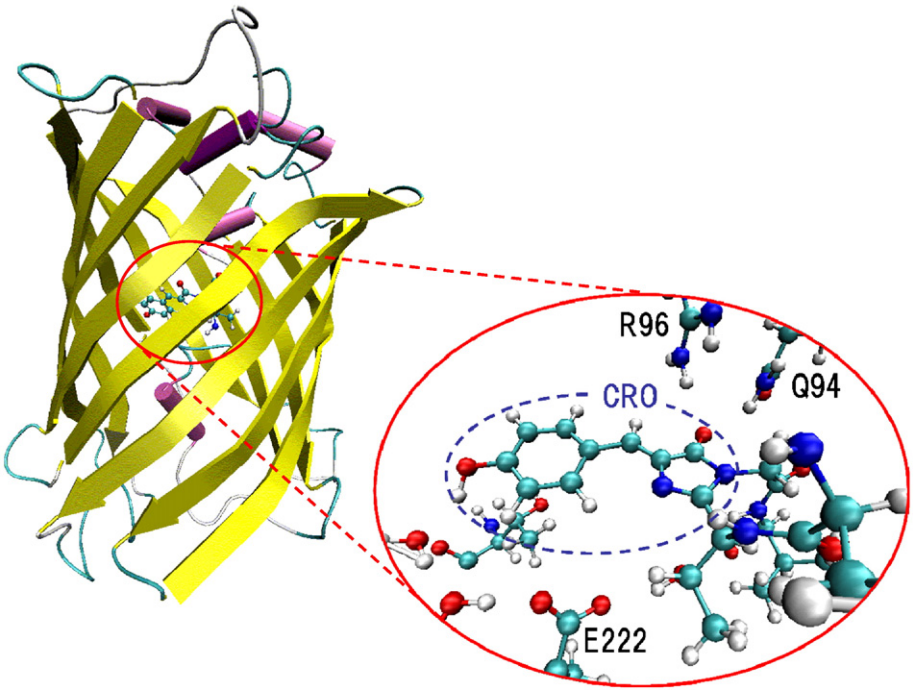

Fig. 1. Ribbon diagram of fluorescent protein and Chromophore (CRO) structures. The β-barrel and α-helices are shown in yellow sheets and pink rolls, respectively. The CRO is in the center of β-barrel, and the detailed structure around CRO is shown in the red circle.

calculations to figure out the irreversible mechanism in the absence of oxygen. Finally, we would like to draw our conclusions in Section 4.

2. Computational detail

2.1. Structures of the model system

We have proposed the photoreaction scheme for the GFP based on the imine-forming reaction [19]. Fig. 2 shows the reaction scheme of our model from reactant structure (I : GFP model) to the formation of the Schiff-base between R96 and CRO (III : RsFP model) via intermediate structure (II : Intermediate model). We consider only an anionic state of CRO model and the terminally-methylated model structures, because it is well known that the neutral state of CRO becomes the anionic state in the excited state except for atypical mutants like T203I. We have focused on only nucleophilic addition reaction as the rate-determined step in this photoreaction, because the transition energy of the dehydration reaction is usually lower than that of the nucleophilic addition reaction under the condition of protein [25].

In addition, we have also proposed the partial model consisting of the residues with the hydrogen-bonding network around the CRO. This partial model includes V61, T62, T63, F64, CRO, Q94, R96, Y145, N146, S147, H148, I167, R168, H169, Q183, T203, S205, E222, and water 6, 12, 19, and 27 in 1EMB PDB data, as shown in Fig. 3. Some α-carbons of acral residues were substituted methyl group in this model.

2.2. Molecular orbital and molecular dynamics

To confirm the validation of Schiff-base model, *ab initio* MO calculations were performed with the GFP model and RsFP model using Gaussian 03 program packcage [23]. These model structures on the ground (S_0) state were optimized by second-order Møller–Plesset perturbation (MP2) using 6-31G* Gaussian basis set. The vertical excitation energies were calculated by configuration interaction single with perturbative doubles method (CIS(D)) [24] using 6-31G* Gaussian basis set for these optimized structures. Next, MO calculations were performed on the nucleophilic addition reaction between the GFP model and Intermediate model. The GFP model, Intermediate model, and transition state (TS : as shown in Fig. 4) between them were optimized

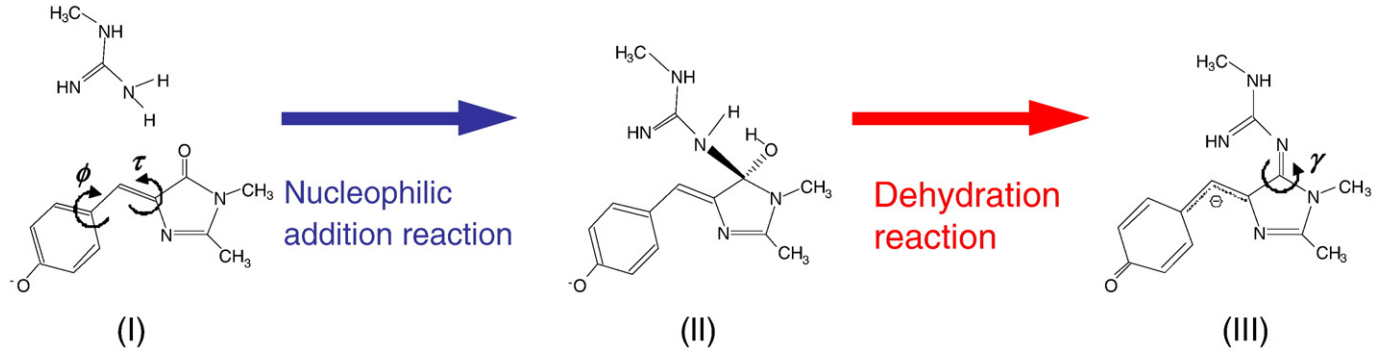

Fig. 2. (I) GFP model picked up R96 and CRO from the 1EMB PDB [18], (II) Intermediate model, and (III) RsFP model of the Schiff-base between R96 and CRO. The dihedral angles ϕ,τ, and γ are also defined.

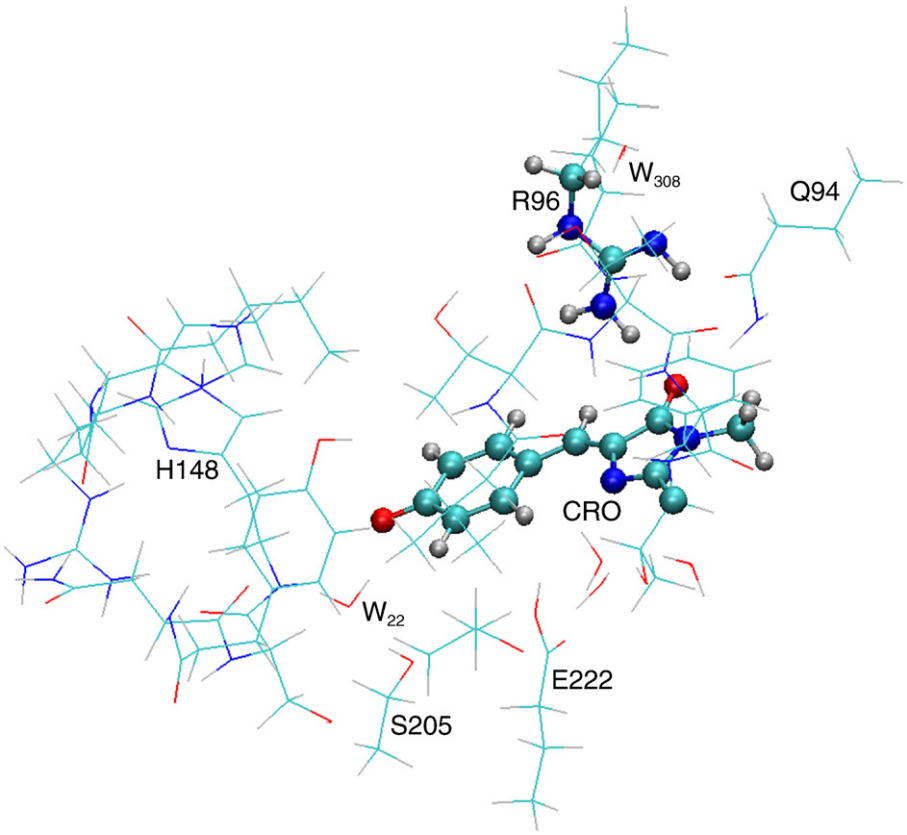

Fig. 3. The partial model consisting of the residues with the hydrogen-bonding network around the CRO. This partial model includes V61, T62, T63, F64, CRO, Q94, R96, Y145, N146, S147, H148, I167, R168, H169, Q183, T203, S205, E222, and water 6, 12, 19, and 27 in 1EMB PDB data.

with HF/6-31G* for ground (S_0) and first excited triplet (T_1) states, and CIS/6-31G* level for first excited singlet (S_1) state. The vertical excitation energies under each optimized structures were also calculated with CIS/6-31G* level. To analyze the electrostatic interaction with neighboring residues in the protein environment, we calculated the partial models corresponding to above models (I and TS). The structure of the CRO and R96 was fixed as the optimized geometry of the original CRO model with CIS or HF/6-31G* level, while the structure of other parts in the partial model was optimized with PM3 level. The energy of the partial model was estimated with the ONIOM method, where HF (or CIS)/6-31G* and PM3 levels were employed for the CRO model (only CRO and R96) and other parts, respectively.

We performed the MD calculations of whole GFP with AMBER force field [20,21] using AMBER 9,[26] to analyze the structure and motion of the CRO and residues around CRO on S_0 state. A general AMBER force field (GAFF) [21] was used as a force field for part of CRO. It is noted that the potential energy curve with respect to the internal rotation of CRO is reasonably consistent between the force field and the *ab initio* calculations (HF/6-31G* level). The MD calculations were performed on the system which contains the GFP and about 7000 water molecules (TIP3P [22] force field) at 300 K with the periodic boundary condition. The optimized structure of this system was employed as the initial coordinate. The simulation time is 2.0 ns (2,000,000 steps).

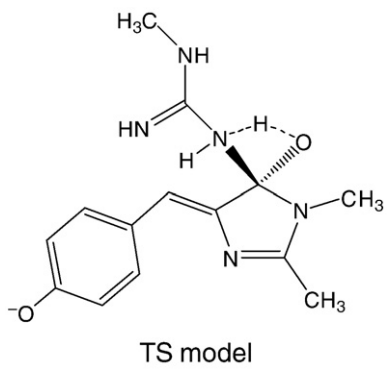

Fig. 4. Transition state model for the addition reaction in red shift reaction. :between (I) the GFP model and (II) Intermediate model.

3. Results and discussion

3.1. Absorption energies of our models

In order to confirm the validation of our models, we have calculated the absorption energies for GFP model and RsFP model, and compared with the corresponding experimental values. We also calculated another RsFP models such as the protonated Schiff-base structure appeared in Retinal (IV), [27] the protonated amino group on R96 (V), and Schiff-base structure between CRO and Q94 (VI), as shown in Fig. 5.

Table 1 shows absorption energies and absorption energy difference between GFP and RsFP. The absorption energies difference between the GFP and RsFP models is 0.21 eV, which is in reasonable agreement with the corresponding experimental value of 0.25 eV. However, the other models (IV–VI) shown in Fig. 5 are not in reasonable agreement with the experimental result. To explain the results, we focus the dihedral angle defined as γ, which corresponds to the planarity of two planes in RsFP models, as shown in Fig. 2. While the γ dihedral angle is almost zero in optimized RsFP model (III), the dihedral angles of the other models (IV–VI) are about 70°. This clearly appears that the red-shift of absorption energy was observed in RsFP model (III) because the conjugated double bonding elongates in only RsFP model (III).

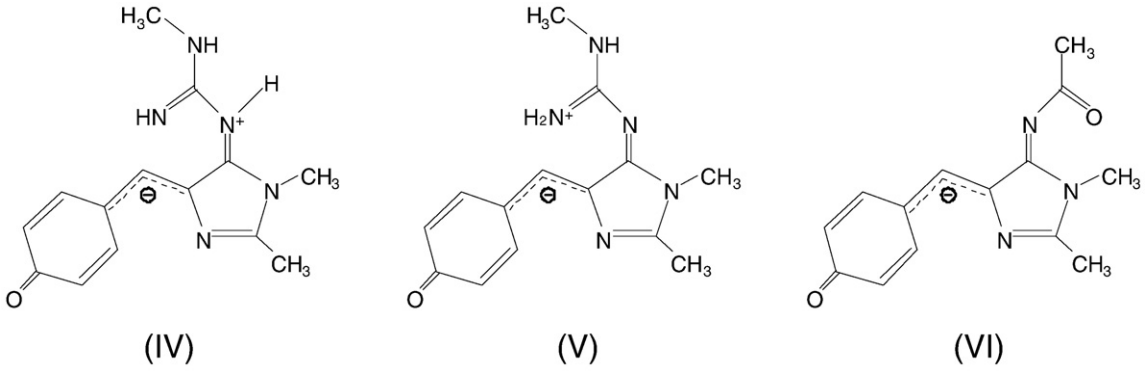

Fig. 5. Three different RsFP-models; (IV) protonated Schiff-base, (V) protonated amino group on R96, and (VI) Schiff-base between CRO and Q94.

3.2. Analysis of GFP photoactivation reaction pathway

The nucleophilic addition reaction is considered as the rate-determined step in the formation of Schiff-base under the protein condition [25]. The GFP model (I), Intermediate model (II), and TS structure were optimized for S_0, S_1, and T_1 states along the nucleophilic addition reaction. Table 2 shows relative energies of S_0, S_1, and T_1 for optimized structures on each states, relative to the S_0 energy of the GFP model optimized in S_0 state. The lowest reaction energy barrier on S_1 state is 2.81 eV, which corresponds to the energy difference between the S_1 energy of TS structure optimized S_1 state (6.82 eV) and vertical excitation energy from S_0 to S_1 in GFP model (I) optimized S_0 state (4.01 eV), in this nucleophilic addition reaction after the photoexcitation. The relative energy of TS structure in T_1 state, even in the lowest energy on the optimized T_1 state (4.34 eV), is 0.33 eV higher than the vertical excited energy from S_0 to S_1 in S_0-optimized structure (4.01 eV).

From the ONIOM calculation with the partial models of I and TS, we obtained the vertical excitation energy of 3.93 eV from S_0 state to S_1 state for the partial model of reactant, while the relative T_1 energy of 3.23 eV for the partial model of TS. This result clearly demonstrated that the energy barrier on the reaction pathway through T_1 state was vanished in the environment of the neighboring residues. We also observed the slight deviation of Mulliken population on atoms in the CRO between the original CRO model and the partial model. The remarkable deviations of Mulliken population are of the oxygen ($\delta-$: -0.05) and carbon ($\delta+$: 0.09) of carbonyl group on imidazole ring, and nitrogen ($\delta-$:-0.09) of amino group on R96. Such charge deviation should accelerate the addition reaction of imine-forming, and thus the energy of T_1 state in protein environment becomes to be lower than that in the original CRO model.

On the basis of above results, after excitation from S_0 state to S_1 state, CRO immediately turns to T_1 state in the absence of oxygen. As the first step of the red-shift reaction of GFP, thus, the nucleophilic addition reaction would occur to form the new σ-bond between R96 (the nucleopetal nitrogen atom of amino group) and CRO (the electrophilic carbon atom of carbonyl group) with the proton transfer between the nitrogen atom of the amino group and the oxygen atom of the carbonyl group. The second step of the dehydration reaction to form Schiff-base should be fast [25].

It is well known that the ϕ and τ dihedral angles in Fig. 2 can rotate in excited states, [9] which is important in production and decay of the fluorescent state [10–13]. To see the planarity of CRO, Vendrell et al. [5] focused on the dihedral angle between the two rings in the CRO (θ). We have also focused on θ in each states. The value of θ of (I) GFP model and (II) Intermediate model almost keep the CRO-planarity for S_0 state (0.6 and 6.3 degree, respectively), while the dihedral angles of them for S_1 state are 10.2 and 70.6 degree and for T_1 state are 3.7 and 52.7 degree, respectively.

Fig. 6 shows the histogram of θ on S_0 state with our MD simulation at 300 K. The solid line in the Fig. 6 is the Gaussian fitted function approximated as the normal distribution. The standard deviation (σ) of the Gaussian function is 12.3° and the median (μ) is -3.0°. Actually, the vibrational frequency of the dihedral angle of ϕ is $\sim 70\ \mathrm{cm}^{-1}$ within HF/6-31G* level. Vendrell [5] reported that the distribution of θ has two peak, while our result shows the single peak distribution.

Our results show that θ is widely distributed in S_0 state, and the dihedral angles of S_1 (10.2°) and T_1 (3.7°) in each optimized structures

Table 1
Theoretical and experimental absorption energies (ΔE), and absorption energy difference between GFP and RsFP ($\Delta\Delta E$). The unit is in eV.

		Form	ΔE	$\Delta\Delta E$
Our results	GFP model	I	2.87	–
	RsFP model	III	2.66	0.21
		IV	3.80	−0.93
		V	3.88	−1.01
		VI	2.79	0.08
Exptl.[14]	GFP		2.61	–
	RsFP		2.36	0.25

Table 2
Relative energies of S_0, S_1, and T_1 states with optimized structures in each state. The unit is in eV.

	S_0-optimization			S_1-optimization			T_1-optimization		
	I	TS	II	I	TS	II	I	TS	II
S_0	0.00	3.14	2.06	0.15	3.24	5.22	0.33	3.50	4.04
S_1	4.01	6.90	6.32	3.90	6.82	5.41	4.03	6.94	6.21
T_1	2.15	4.56	3.80	2.04	4.42	3.35	2.18	4.34	3.06

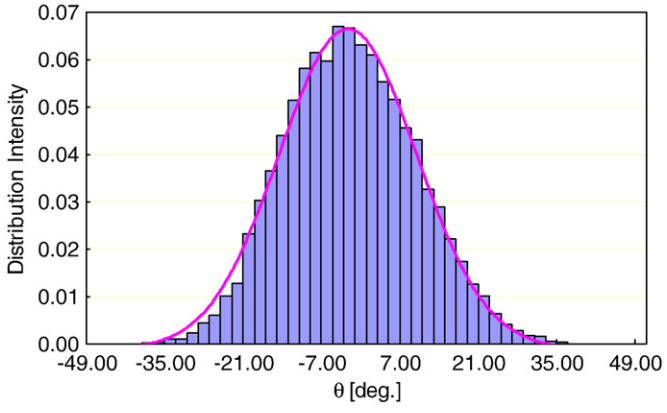

Fig. 6. Histogram of the CRO ring-ring dihedral angle (θ). The solid line is the Gaussian fitting function. The value of median (μ) is -3.0° and of deviation (σ) is 12.3°.

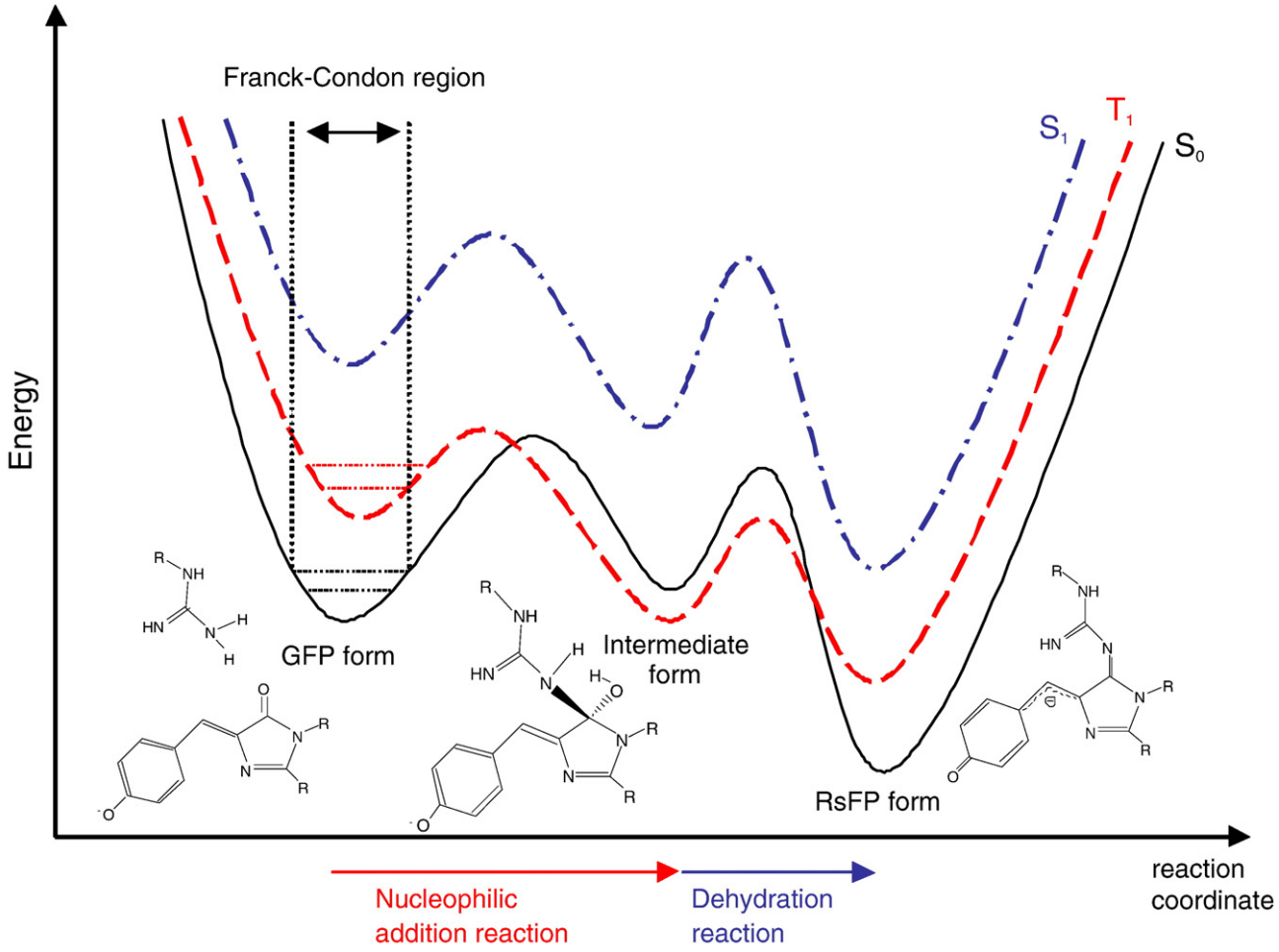

Fig. 7. Schematic diagram of GFP photoactivation reaction under the protein condition. First step is the nucleophilic addition reaction. Second step is the dehydration reaction to form Schiff-base on T_1 state.

of the GFP model exist within the thermal vibration at 300 K. There is little change in the others degree of freedom. This structural information partly supports that the CRO excited from S_0 state to S_1 state turns to T_1 state in GFP photoactivation, and nucleophilic addition reaction occurs on the T_1 state. If the nucleophilic addition reaction occurs on S_1 state, the structure would return to GFP model structure rapidly in the relaxation from S_1 state to S_0 state. Namely, this nucleophilic addition reaction occurs by turning to only T_1 state. This results support the experimental results that GFP photoactivation occur only in the absence of oxygen [14,15]. On the basis of these results, we show the schematic diagram of GFP photoactivation reaction in Fig. 7, although the part of dehydration reaction in GFP red-shift behavior is just speculated.

We cannot discuss quantitatively because the energies were calculated with HF and CIS level of calculation for simple models. However, our results show that the optimized structures of GFP model for S_1 and T_1 states would exist within the Franck-Condon region at 300 K. We also show the irreversible red-shift reaction of GFP under the absence of oxygen, because the CRO excited from S_0 state to S_1 state immediately turns to T_1 state, and nucleophilic addition reaction occurs on T_1 state.

4. Conclusion

We have proposed the photoreaction mechanism of GFP as the formation of Schiff-base between R96 and CRO. The difference between the absorption energies of RsFP model (Schiff-base model) and GFP model with CIS(D)/6-31G* level is 0.21 eV, which is in reasonable agreement with the corresponding experimental value of 0.25 eV. We found that the ring-ring dihedral angles of the optimized structures of the GFP model in S_1 and T_1 states exist within the thermal vibration at 300 K. We show that the T_1 pathway has an advantage over the S_1 pathway in this nucleophilic addition reaction. We conclude finally that GFP red-shift reaction is irreversible because the CRO excited from S_0 state to S_1 state immediately turns to T_1 state, and nucleophilic addition reaction occurs in T_1 state.

Acknowledgment

We thank Professor Umpei Nagashima and Dr. Takayoshi Ishimoto for their useful discussion. This study was supported by a Grant-in-Aid for Scientific Research and for the Priority Area by the Ministry of Education, Culture, Sports, Science, and Technology.

References

[1] O. Shimomura, F.H. Johnson, Y. Saiga, J. Cell. Comp. Physiol. 59 (1962) 223.
[2] A.A. Pakhomov, V.I. Martynov, Chem. Biol. Rev. 15 (2008) 755.
[3] R.Y. Tsien, Annu. Rev. Biochem. 67 (1998) 509.
[4] J. Bacteriol, Biophys. J. 88 (2005) 2452.
[5] O. Vendrell, R. Ggelabert, M. Moreno, J.M. Lluch, J. Am. Chem. Soc. 128 (2006) 3564.
[6] S. Wang, S.C. Smith, Phys. Chem. Chem. Phys. 9 (2007) 452.
[7] C. Manca, Chem. Phys. Lett. 443 (2007) 173.
[8] O. Vendrell, R. Ggelabert, M. Moreno, J.M. Lluch, J. Phys. Chem. 112 (2008) 5500.
[9] M. Zimmer, Chem. Rev. 102 (2002) 759.
[10] W. Weber, V. Helms, J.A. Mccammon, P.W. Langhoff, Proc. Natl. Acad. Sci. USA 96 (1999) 6177.
[11] M.C. Chen, C.R. Lambert, J.D. Urgitis, M. Zimmer, Chem. Phys. 270 (2001) 157.

[12] M.E. Martin, F. Negri, M. Olivucci, J. Am. Chem. Soc. 126 (2004) 5452.
[13] P. Altoe', F. Bernardi, M. Garavelli, G. Orlandi, F. Negri, J. Am. Chem. Sos. 127 (2005) 3952.
[14] M.B. Elowitz, M.G. Surette, P.-E. Wolf, J. Stock, S. Leibler, Curr. Biol. 7 (1997) 809.
[15] M.B. Elowitz, M.G. Surette, P.-E. Wolf, J.B. Stock, S. Leibler, J. Bacteriol 181 (1999) 197.
[16] M.V. Matz, A.F. Fradkov, Y.A. Labas, A.P. Savitsky, A.G. Zaraisky, M.L. Markelov, S.A. Lukyanov, Nature Biotech. 17 (1999) 969.
[17] R. Ando, H. Hama, M. Yamamoto-Hino, H. Mizuno, A. Miyawaki, Proc. Natl. Acad. Sci. USA 99 (2002) 12651.
[18] K. Brejc, T.K. Sixma, P.A. Kitts, S.R. Kain, R.Y. Tsien, M. Ormö, S.J. Remington Proc, Natl. Acad. Sci. USA 94 (1997) 2306.
[19] J. McMurry, T. Begley, The Organic Chemistry of Biological Pathways, Roverts and Company Publishers, 2005.
[20] J. Wang, P. Cieplak, P.A. Kollman, J. Comp. Chem. 21 (2000) 1049.
[21] J. Wang, R.M. Wolf, J.W. Caldwell, P.A. Kollman, D.A. Case, J. Comp. Chem. 25 (2004) 1157.
[22] W.L. Jorgensen, J. Chandrasekhar, J.D. Madura, R.W. Impey, M.L. Klein, J. Chem. Phys. 79 (1983) 926.
[23] M.J. Frisch, G.W. Trucks, H.B. Schlegel, et al., GAUSSIAN 03, Gaussian, Inc, Wallingford, CT, 2004.
[24] M. Head-Gordon, R.J. Rico, M. Oumi, T.J. Lee, Chem. Phys. Lett. 219 (1994) 21.
[25] W.P. Jencks, Catalysis in Chemistry and Enzymology, McGraw-Hill, New York, 1969.
[26] D.A. Case, T.A. Darden, T.E. Cheatham III, et al., AMBER 9, 9th ed., University of California, San Francisco, 2006.
[27] B. Honing, A.D. Greenberg, U. Dinur, T.G. Ebrey, Biochem. 15 (1976) 4593.